'94 KACC (1994. 10. 17 ~ 20)

Precise Positioning H∞ Control Considering Resonance and Coulomb Friction

A. Yamauchi, Y. Mikami, A. Moran and M. Hayase
Faculty of Eng., Tokyo Univ. of Agric. & Technology
Koganei-shi, Tokyo 184, Japan

Abstract

The control system of a precise positioning mechanism with resonance and Coulomb friction has been designed using H∞ control theory, and the control performance has been verified by computer simulation and experimental analysis. The DGKF type H∞ control theory with scalar weighting factors was utilized for designing the control system.

The followings have been confirmed from the present study:

(1) The system with H∞ control presents better convergence and stability than the system with conventional control (PI-notch filter control).

(2) The H∞ control system have good robustness properties for a wide range of operating conditions in the presence of external disturbances such as Coulomb friction and changing mechanical resonant frequency.

1. Introduction

A precise positioning system considering mechanical resonance and Coulomb friction has been designed on the basis of H∞ control theory. Positioning control is being studied actively in many manufacturing fields in order to improve the accuracy and performance of manufacturing process. Certain behavior is desirable in positioning control systems-fast convergence, small steady state error, and robustness are desirable properties of positioning control systems operating under the presence of external disturbances such as Coulomb friction and changes in the system parameters.

Steady state error performance can not be directly taken into consideration in DGKF type H∞ control theory. Solid friction, which exists in most of positioning mechanisms, disturbs the control characteristics and negatively affects the precision and accuracy of the system. It is therefore essential to use a Type-1 compensator since lasting disturbances such as friction are always present in positioning control.

The following points were considered for designing the compensator analyzed in this paper:

(1) H∞ control theory is utilized to design a control system with the desired convergence and robustness properties.

(2) In order to suppress the negative effects of Coulomb friction, it was modeled as one of the disturbances of the H∞ control system.

(3) The frequency and step responses of the positioning control system were analyzed theoretically and experimentally. The experimental step response was obtained considering milimeter-order translations and a mechanical resonant frequency of 5 Hz. These values were selected to perform the experimental analysis with ease and to study the feasibility of compensating for the effects of Coulomb friction and changes in the system and its environment.

2. Experimental system

Figure 1 shows the fundamental structure of the vibrational model of the precise positioning mechanism[1]. A DC motor rotates a ballscrew, and the ballscrew actuates a positioning stage which has longitudinal motion. There are friction forces and friction torque affecting the DC motor and the positioning stage, respectively. Figure 2 shows the experimental setup. A DC motor rotates according to a control voltage, turns a ballscrew to linearly move a sub-stage attached to the main stage through two plate springs.

The DC motor and ballscrew had friction torque, and the sub-stage is affected by friction forces. The friction at the sub-stage could be varied. According to the difference between the present position of the sub-stage and the desired position, a control voltage V_I is calculated by a computer and send to a power amplifier to control the DC motor.

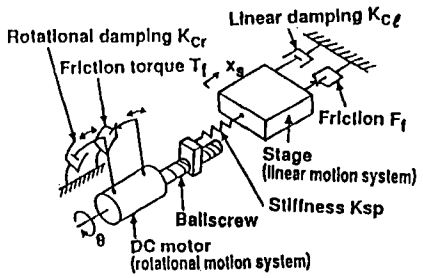

Fig. 1 Vibrational model of positioning mechanism

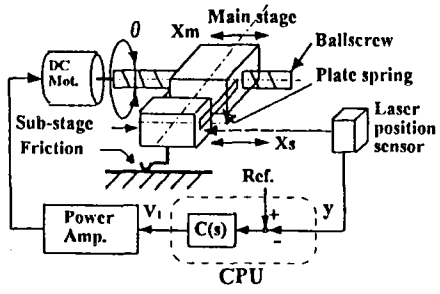

Fig. 2 Experimental system

3. Modeling and Identification

3-1. Motion equations

The motion equations of the electrical system in the DC motor and amplifier can be described as follows :

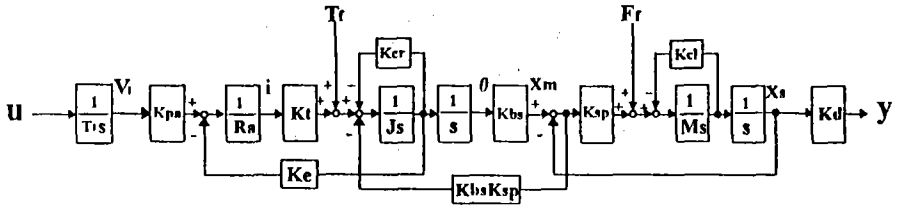

Fig. 3 Block diagram of positioning system

$$K_{pa}V = K_e \frac{d\theta}{dt} + Ri \qquad \cdots ①$$

The above equation neglects the inductance of DC motor to simplify the controller design.

The rotational motion equations of the drive mechanism can be described as follows :

$$T - T_f - T_{qr} = J\frac{d^2\theta}{dt^2} + K_{cr}\frac{d\theta}{dt} \qquad \cdots ②$$

where T_f is the Coulomb friction torque which nonlinearly depends on $d\theta/dt$ as shown in Figure 4.

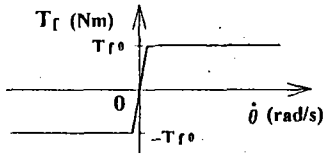

Fig. 4 Modeling of Coulomb friction torque

T_{qr} is an equivalent torque representing the effect of the rotational motion of the main stage and is equal to :

$$(x_m - x_s)K_{sp}K_{bs}$$

The linear motion equations of the sub-stage can be described as follows :

$$(x_m - x_s)K_{sp} - F_f = M\frac{d^2x_s}{dt^2} + Kcl\frac{dx_s}{dt} \qquad \cdots ③$$

The detectable output is :

$$y = K_d x_s \qquad \cdots ④$$

where K_d is the gain of the laser sensor.

Figure 3 shows the block diagram of the complete positioning mechanism based on equations ① to ④.

Table 1 shows the specification of parameters and nomenclature.

Table 1 List of individual parameters

Kpa	Power amplifier gain	10
Ra	DC motor resistance	1.1 ohm
Kt	DC motor torque constant	0.0573 Nm/A
Ke	Back electromotive force const	0.0567 Vs/rad
J	Moment of inertia	0.0453 g
Kcr	Rotational damoing factor	(0.0045) kgm²/s
Kbs	Ballscrew transducing coefficient	(0.00151) m/rad
l	Lead of ball screw	0.01 m
Ksp	Spring stiffness	(299)N/m
Kcl	Linear damping factor	(0.87) Ns/m
M	Mass of linear damping system	0.244 kg
Kd	Position sensor coefficient	50 V/m
Tf0	Friction torque	0.037 Nm
Ff0	Friction force	0.01 N

3-2. Parameter identification

The most of parameters of the system (such as K_{pa}, R_a, K_t, K_e, J, K_{bs}, l, M, and K_d) can be directly measured or calculated. The other parameters (K_{sp}, K_{cl}, and K_{cr}) are determined from the experimental response of the system : K_{sp} is determined from the resonant frequency of the system, K_{cl} is determined from the declining oscilation of the step response and K_{cr} is determined so that the theoretical and experimental frequency responses of the open-loop system agree.

3-2-1. Frequency response

Figure 5 shows the theoretical and experimental frequency responses (gain and phase) of the sub-stage displacement. It can be noted that there is a good agreement between theoretical and experimental responses. The slight difference between both responses is owed to the effect of Coulomb friction.

3-2-2. Transient response

To analize the transient response of the system, the input voltage to the DC motor was chosen to be as shown in Figure 6. Figure 7 compares the theoretical and experimental transient responses of the positioning mechanism. It can be noted that there is a good agreement between both responses. Given to the effect of Coulomb friction, the experimental transient response does not last as the calculated response.

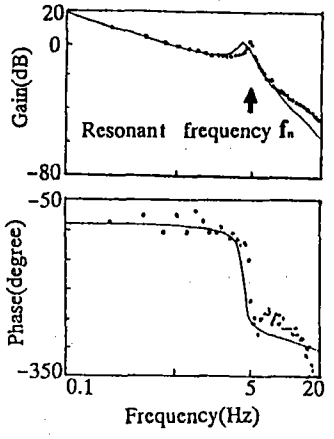

- Simulation · Experiment

Fig.5 Frequency response of positioning system (open-loop)

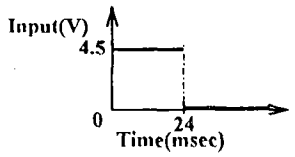

Fig. 6 Input voltage

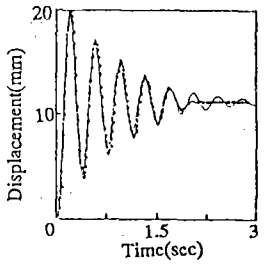

– Simulation · Experiment

Fig. 7 Transient response of positioning system (open-loop)

4. H∞ control theory

In this study, the control system has been designed according to the DGKF type H∞ control theory[6]. This theory has been developed from LQG control theory in which disturbances and control variables are treated explicitly. Feedback and observer gains are obtained by solving two Riccati equations. The basic block diagram of the system with H∞ control is shown in Figure 8.

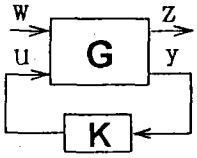

Fig.8 Basic block diagram of system with H∞ control

In Figure 8, G stands for the generalized plant, K is the controller, u is the control input, y is the measured variable, z represents the controlled variable, and w is the disturbance vector. According to the H∞ control method, a controller is designed so that the H∞ norm of the closed-loop transfer function T_{zw} from disturbances to controlled variables is less than γ. That is :

$$\|T_{zw}\|_\infty < \gamma \qquad \cdots ⑤$$

The effect of the disturbance on the controlled variables is reduced by choosing the smaller value of γ.

The generalized plant G is described by the equations :

$$\begin{aligned} \frac{dx}{dt} &= Ax + B_1 w + B_2 u \\ z &= C_1 x + D_{11} w + D_{12} u \\ y &= C_2 x + D_{21} w + D_{22} u \end{aligned} \qquad \cdots ⑥$$

where x is the state vector which includes the state variables of the actual system and other variables representing weighting functions, integral action etc..

The following assumptions are required to design a controller according to DGKF H∞ control theory :

(Ⅰ) $[A, B_1]$ stabilizable and $[C_1, A]$ detectable

(Ⅱ) $[A, B_2]$ stabilizable and $[C_2, A]$ detectable

(Ⅲ) $D_{11} = 0$ and $D_{22} = 0$ $\cdots ⑦$

(Ⅳ) $D_{12}^T C_1 = 0$ and $D_{12}^T D_{12} = I$

(Ⅴ) $B_1 D_{21}^T = 0$ and $D_{21} D_{21}^T = I$

The H∞ controller can then be written as

$$\frac{d\hat{x}}{dt} = \hat{A}\hat{x} - ZLy \quad u = F\hat{x}$$

where

$$\begin{aligned} \hat{A} &= A + \gamma^{-2} B_1 B_1^T X + B_2 F + ZLC_2 \\ F &= -B_2^T X, \; L = -YC_2^T \\ Z &= (I - \gamma^{-2} YX)^{-1} \end{aligned} \qquad \cdots ⑧$$

$\hat{x}$ is the estimate of x, and X and Y are the positive solutions of the following Riccati equations:

$$A^T X + XA + C_1^T C_1 + X\left[\gamma^{-2} B_1 B_1^T - B_2 B_2^T\right] X = 0 \qquad \cdots ⑨$$

$$AY + YA^T + B_1 B_1^T + Y\left[\gamma^{-2} C_1^T C_1 - C_2^T C_2\right] Y = 0 \qquad \cdots ⑩$$

The spectral radius of the product XY must be less than γ^2 :

$$\rho(XY) < \gamma^2 \qquad \cdots ⑪$$

5. Generalized plant

In order to eliminate steady-state errors originated by friction, integral action was added to the controlled system as shown in Figure 9, where P(s) is the positioning mechanism with power amplifier, K(s) is the compensator, and T_I is the integral time constant. The descriptions of all the matrices of the generalized plant are shown in Equation ⑫. Although K(s) is the compensator of the generalized plant, the compensator of the actual system is $C(s) = K(s)/T_I s$.

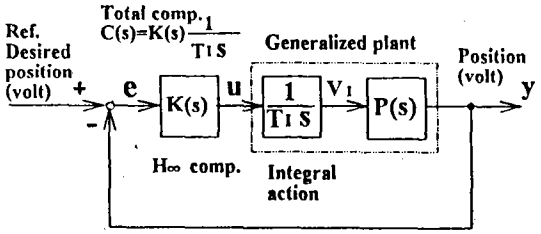

Fig. 9 H∞ control system with integral action

$$A = \begin{bmatrix} 0 & 0 & 0 & 0 & 0 \\ \frac{K_t K_{pa}}{R_a J} & -\frac{K_a R_a + K_t K_e}{R_a J} & -\frac{K_{bv}^2 K_{vp}}{J} & 0 & \frac{K_{vp} K_{bv}}{J} \\ 0 & 1 & 0 & 0 & 0 \\ 0 & 0 & \frac{K_{bv} K_{vp}}{M} & -\frac{K_d}{M} & \frac{K_{vp}}{M} \\ 0 & 0 & 0 & 1 & 0 \end{bmatrix}$$

$$B_1 = \begin{bmatrix} \frac{1}{T_I} & 0 & 0 & 0 & 0 & 0 \\ 0 & -\frac{b_2}{J} & 0 & 0 & 0 & 0 \\ 0 & 0 & 0 & 0 & 0 & 0 \\ 0 & 0 & 0 & -\frac{b_1}{M} & 0 & 0 \\ 0 & 0 & 0 & 0 & 0 & 0 \end{bmatrix}$$

$$B_2 = \begin{bmatrix} \frac{1}{T_I} \\ 0 \\ 0 \\ 0 \\ 0 \end{bmatrix}$$

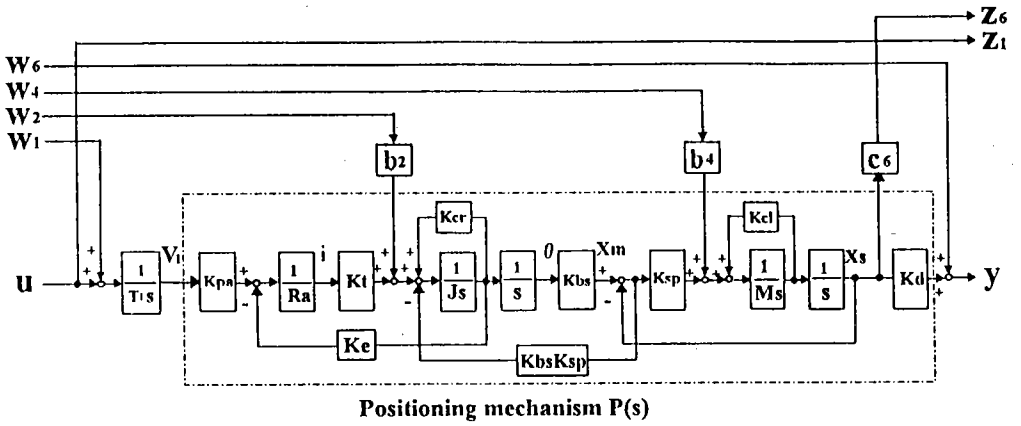

Fig. 10 Block diagram of generalized plant

$$\begin{bmatrix} 0 & 0 & 0 & 0 & 0 \\ 0 & 0 & 0 & 0 & C_6 \end{bmatrix} \begin{bmatrix} 0 & 0 & 0 & 0 & 0 \\ 0 & 0 & 0 & 0 & 0 \end{bmatrix} \begin{bmatrix} 1 \\ 0 \end{bmatrix}$$

$$\begin{bmatrix} 0 & 0 & 0 & 0 & K_4 \end{bmatrix} \begin{bmatrix} 0 & 0 & 0 & 0 & 1 \end{bmatrix} \begin{bmatrix} 0 \end{bmatrix} \quad \cdots (12)$$

Figure 10 shows the block diagram of the generalized plant. The control input u and sub-stage displacement X_s are the controlled variables Z_1 and Z_6, respectively. W_1 and W_6 are the input side noise and the sensor noise, respectively. W_2 and W_4 are the disturbances of friction torque and friction force, respectively. b_2,b_4, and c_6 are weighting factors. The H∞ compensator was designed by choosing optimal values of the weighing factors.

6. Simulation

In order to examine the performance of the positioning system with H∞ control, frequency and step responses of the sub-stage motion were analyzed. The response of the system with H∞ control was compared with the response obtained when a PI compensator with notch filter is used.

6-1. Bode plots

Figure 11 shows the open-loop characteristics of the positioning mechanism. Here, f_n is the mechanical resonant frequency. Figures 12 and 13 show the bode plots of the H∞ and PI-notch filter compensators, respectively. It is noted that for both compensators the gain of the bode plots decrease arround the resonant frequency of the system (5Hz). However, the H∞ controller presents a smoother frequency response. Figures 14 and 15 show the bode plots of the closed-loop transfer function. The closed loop transfer function of the system with H∞ compensator has higher cut-off frequency which mean a better performance for a wide range of frequencies.

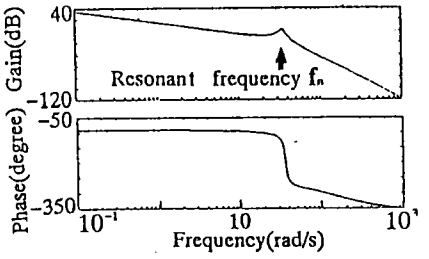

Fig. 11 Bode plot of plant P(s)

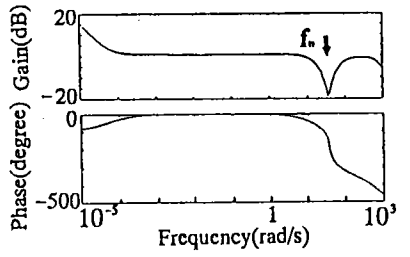

Fig. 12 Bode plot of H∞ compensator

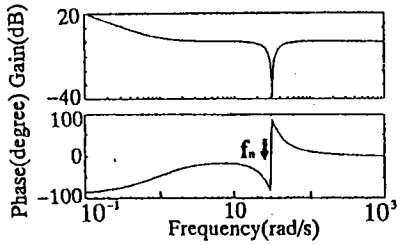

Fig.13 Bode plot of PI-notch filter compensator

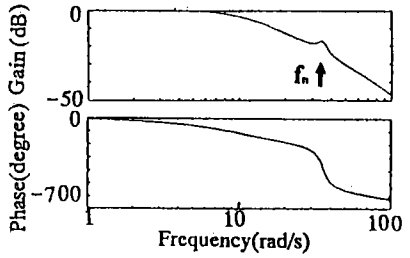

Fig. 14 Bode plot of closed-loop transfer function using H∞ control theory

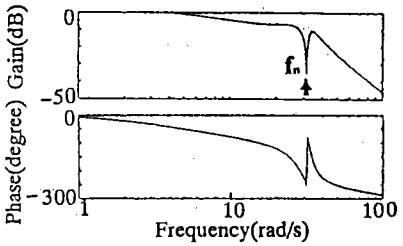

Fig. 15 Bode plot of closed-loop transfer function using PI-notch filter compensator

6-2. Step responses

6-2-1. Response of nominal system

Figures 16 and 17 show the step responses of the closed-loop system using H∞, and PI-notch filter compensator. The step response of H∞ control had better convergence than that of conventional PI-notch filter control. Under conventional PI control, the step response took a long time to converge.

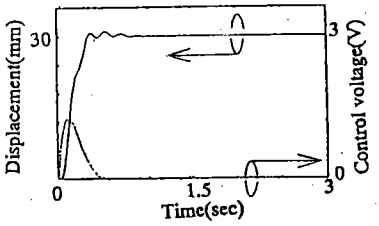

Fig.16 Step response using H∞ control theory

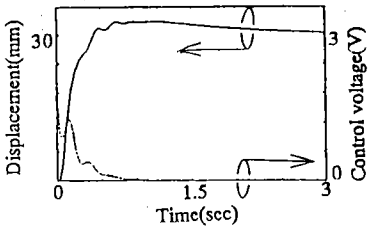

Fig.17 Step response using PI-notch filter control theory

6-2-2. Response when changing the mechanical resonant frequency

Figures 18 and 19 show the step responses of the H∞ and PI-notch filter control when the sub-stage mass has been increased by 20%. While the step response of the system with PI-notch filter varied and oscillations arose, the step response of the system with H∞ control did not vary much. These results verify the robustness properties of the H∞ compensator.

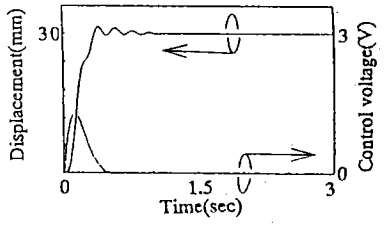

Fig.18 Step response using H∞ control theory when changing resonant frequency

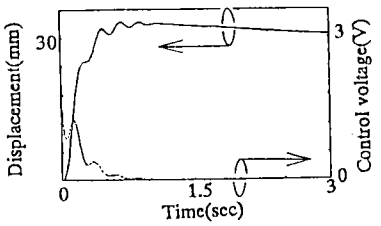

Fig.19 Step response using PI-noch filter control theory when changing resonant frequency

6-2-3. Response when the friction forces are modified

Figures 20 and 21 show the step responses of the H∞ control and PI-notch filter control with friction as variable parameter. The step response of PI-notch filter control oscillated when the friction was decreased to 0.1 times its nominal value and the speed of response fell when the friction was increased to 5 times. On the other hand, the step response of H∞ control varied little as the friction was changed.

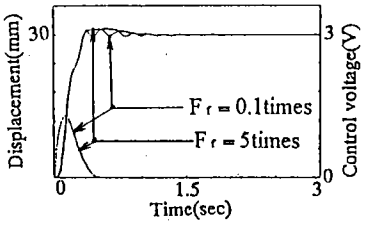

Fig. 20 Step response using H∞ control theory when changing friction

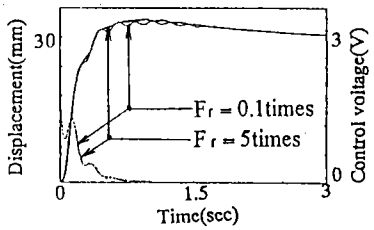

Fig. 21 Step response using PI-notch filter control when changing friction

7. Experimental results (step response)

7-1. Response of nominal system

Figures 22 and 23 show the step responses using H∞ and PI-notch filter control methods. Experimental results show clearly the different features of both control methods under the influence of friction disturbances. These results show that the speed of response using H∞ control is faster than that of PI-notch filter control. In addition, mechanical resonance vibrations were better damped by H∞ control than by PI-notch filter control.

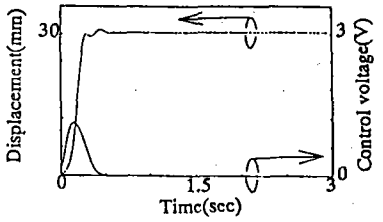

Fig. 22 Experimental step response using H∞ control theory

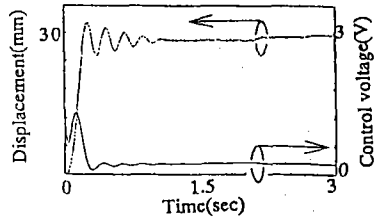

Fig. 23 Experimental step response using PI-notch filter control

7-2. Response when changing the resonant frequency

Figures 24 and 25 show the step responses using H∞ and PI -notch filter control methods when the sub-stage mass has been increased 20%. The experimental results are similar to the calculated results shown in Figures 18 and 19. The step response of PI-notch filter control varied, and oscillations arose when the mass was increased, while the step response of H∞ control did not vary much.

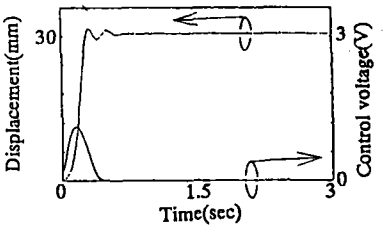

Fig.24 Experimental step response using H∞ control theory when changing resonant frequency

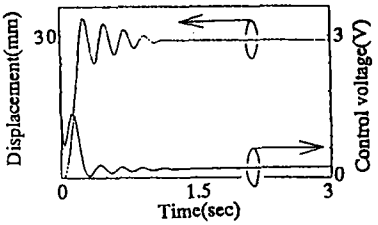

Fig.25 Experimental step response using PI-notch filter control when changing resonant frequency

7-3. Response when changing friction values

Figures 26 and 27 show the step responses using H∞ and PI-notch filter control when changing friction coefficient to 0.1 and 5 times of its nominal value. When decreasing friction, the linear damping factor K_d became smaller, therefore the difference between nominal and friction-changed plant around the resonance frequency became larger. Consequently the resonance oscillations arose when the friction was decreased. The system with H∞ control presents oscillations with smaller amplitude than the system with PI-notch filter control.

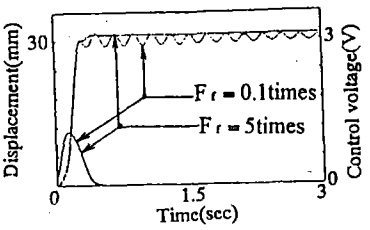

Fig.26 Experimental step response using H∞ control theory when changing friction value

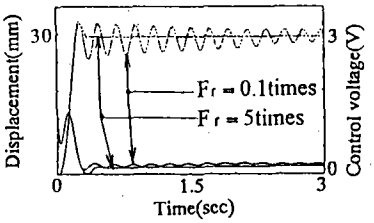

Fig.27 Experimental step response using PI-notch filter control when changing friction value

8. Conclusions

A positioning control system taking into account mechanical resonance and Coulomb friction has been designed according to DGKF type H∞ control theory. Main disturbances such as Coulomb friction were modeled and an augumented plant with integral action was formulated. The followings has been confirmed from the simulation and experimantal results.

(1) H∞ control presents better convergence and stability properties than conventional control (PI with notch filter).

(2) H∞ control has good robustness for all the range of operating conditions even if there exist disturbances such as Coulomb friction and changes in the parameters of the system and its environment.

Acknowledgment

The authors would like to express their sincere thanks to Y.Takahashi of Toshiba Corporation and T.Yamazaki and T.Murakami for their suggestions and help to carry out the experimental work.

References

[1] Y. Takahashi and N. Uchida, Rev. Sci. Instrum., 61, (1990).

[2] Y. Takahashi, A. Yamauchi, S. Mori and M. Hayase, Proc. A-PVC, 1054 (1993).

[3] A. Yamauchi, Y. Mikami, Y. Takahashi and M. Hayase, The 71th Spring Annual meeting of JSME, 513, (1994).

[4] A. Yamauchi, Y. Mikami, Y. Takahashi and M. Hayase, The 33rd SICE Annual Conference, 295, (1994).

[5] Y. Takahashi, A. Yamauchi, Y. Mikami, and M. Hayase, Proc. of MOVIC, (1994).

[6] J. C. Doyle, K. Glover, P. P. Khargonekar, and B. A. Francis, IEEE, Trans. Auto. Contr., 34, 831 (1989).